NUCLEAR THEORY, Vol. 38 (2019)
eds. M. Gaidarov, N. Minkov, Heron Press, Sofia

Toroidal Mode in Nuclei: Recent Progress

V.O. Nesterenko[1], **J. Kvasil**[2]

[1]Laboratory of Theoretical Physics, Joint Institute for Nuclear Research, Dubna, Moscow region, 141980, Russia

[2]Institute of Particle and Nuclear Physics, Charles University, CZ-18000, Praha 8, Czech Republic

Abstract. We review the recent progress in exploration of the vortical toroidal dipole resonance (TDR). For the particular case of the spherical nucleus ^{140}Ce, the interplay of TDR and irrotational pygmy dipole resonance (PDR) is analyzed within the Skyrme quasiparticle random-phase approximation (QRPA) method. For this aim, the dipole strength functions, transition densities, and current distributions are inspected. We also present some arguments to justify TDR as a general feature of atomic nuclei.

1 Introduction

Nuclear excitations can be separated into two groups: irrotational with $\vec{\nabla}\times\vec{j}=0$ (where $\vec{j}$ is the nuclear current) and vortical with $\vec{\nabla}\cdot\vec{j}=0$ [1]. The typical examples of irrotational excitations are isoscalar ($T=0$) and isovector ($T=1$) electric giant resonances, e.g. $E1(T=1)$, $E2(T=0,1)$, $E3(T=0,1)$ [2]. The vortical excitations are exemplified by magnetic orbital resonances like the scissors $M1(T=1)$ [3, 4] and twist $M2(T=0,1)$ [5] modes. In the electric channel, the only known vortical mode is the torodal dipole resonance (TDR) see e.g. [6–22]. In the large family of $E1$ excitations (giant dipole resonance (GDR), pygmy dipole resonance (PDR), compression dipole resonance (CDR) and TDR itself), only TDR demonstrates the vortical flow. In Figure 1, where PDR, TDR and CDR nuclear currents are schematically shown, only TDR exhibits the vortical flow which is seen as rotation-like oscillations of nucleons on a torus surface. The vortical flow does not contribute to the continuity equation (CE). So, if we aim to investigate nuclear motion beyond CE, the TDR is just the “doorway” to this still almost unexplored area.

It is believed that TDR and CDR form the low- and high-energy parts of isoscalar giant dipole resonance (IS GDR) [2]. The experimental observation and identification of TDR is not simple. The resonance is usually masked by other multipole modes (including dipole excitations of non-toroidal nature) located in the same energy region. As a result, even the most relevant (α,α') experimental data [23, 24] still do not provide the direct and complete evidence of TDR, see e.g. discussions [20, 25].

Being a remarkable example of the electric vortical motion, the TDR was intensively investigated during last decades, see e.g. reviews [13,19]. In particular, a comprehensive study of various TDR properties was performed within Skyrme quasiparticle random-phase-approximation (QRPA) method by our Dubna–Prague–Bratislava–Erlangen group [14–22, 25–27]. We presented the detailed derivation of the toroidal, compression, and purely vortical operators [14], demonstrated that the main nuclear flow in dipole states in the PDR energy region is toroidal [15], performed a critical analysis of familiar criteria of the nuclear vorticity and proposed the toroidal mode as a robust measure of the vorticity [16], considered peculiarities of TDR in axial deformed nuclei [17, 19, 20], demonstrated basically mean field origin of the toroidal flow [18], performed a systematic analysis of TDR/PDR interplay in Ca, Ni, Zr, and Sn isotopes [26].

As the next important step, we have shown that, in light axial deformed nuclei like ^{24}Mg and ^{20}Ne, there should exist low-energy $E1$ individual toroidal states (ITS) with $K = 1$ (where K is the projection of the total angular momentum to the symmetry z-axis) [21, 22, 25]. As compared with TDR which is usually masked by other excitations, ITS are well separated from the neighboring excitations and so can be much easier observed and identified. ITS were also predicted in ^{10}Be [28, 29], ^{12}C [30], and ^{16}O [31] by Kyoto group using the combined antisymmetrized molecular dynamics + generator coordinate method [32]. Finally, we proposed the prescriptions to identify ITS and TDR in inelastic electron scattering to back angles [25].

One of the most interesting problems concerning TDR is its interplay with PDR. TDR and PDR share the same energy region but have essentially different nuclear flow: vortical in TDR and irrotational in PDR, see Figure 1. The TDR/PDR interplay is important because it can affect the PDR features which, in turn, are essential for various astrophysical problems and construction of the nuclear equation of state [13]. As shown in our studies for ^{208}Pb [15] and Ca, Ni, Zr, and Sn isotopes [26], the 1^- states at the TDR/PDR energy region have basically toroidal nuclear flow. At the same time, they have a minor irrotational fraction resulting in PDR. Just this fraction gives typical PDR transition densities where the neutron contribution dominates over the proton one at the nuclear boundary.

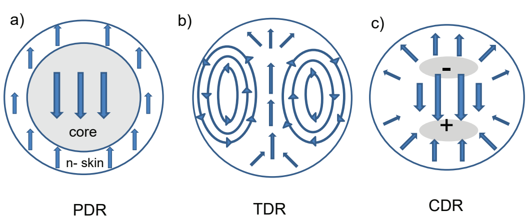

Figure 1. Schematic current fields for PDR (a), TDR (b), and CDR (c). In the plot (c), the compression (+) and decompression (-) regions are marked.

In this paper, we scrutinize the TDR/PDR interplay in the spherical nucleus ^{140}Ce and show that our previous conclusions are valid at the mass region $A \sim 140$ as well. Besides we present some arguments justifying that the vortical toroidal mode is the general feature of atomic nuclei.

2 Calculation Scheme

The calculations for the spherical nucleus ^{140}Ce are performed within the Skyrme QRPA [33]. The method is fully self-consistent since: i) both the mean field and residual interaction are obtained from the same Skyrme functional, ii) both time-even and time-odd densities/currents are involved, iii) the residual interaction includes all the terms of the initial Skyrme functional as well as the Coulomb direct and exchange terms, iv) both ph- and pp-channels in the residual interaction are taken into account. We use Skyrme parametrization SVbas [34] and the surface pairing [35]. The pairing is treated at the BCS level [20]. QRPA employs a large two-quasiparticle (2qp) basis with the energies up to ~ 100 MeV so as the energy-weighted Thomas-Reiche-Kuhn [1] and isoscalar dipole [2] sum rules are almost completely exhausted.

We calculate the dipole strength functions

$$S_X(E1,T;E) = \sum_{\mu}\sum_{\nu} E^{m_X} \left| \langle\nu|\, \hat{M}^X_{1\mu}(T)\, |0\rangle \right|^2 \xi_\Delta(E-E_\nu) \tag{1}$$

where E_ν is the energy of νth QRPA state and E is the energy of the strenth function. Further, $X = \{\mathrm{el}, \mathrm{tor}, \mathrm{com}\}$ denotes dipole transitions (electric ordinary, toroidal, compression). The energy multiplier takes place for $X = \mathrm{el}$ with $m_{\mathrm{el}} = 1$ and is absent for $X = \mathrm{tor}, \mathrm{com}$ with $m_{\mathrm{tor}} = m_{\mathrm{com}} = 0$. We use in (1) the transition matrix elements: ordinary dipole

$$\langle\nu|\, \hat{M}^{\mathrm{el}}_{1\mu}(T=1)\, |0\rangle = \int d\vec{r}\, r Y_{1\mu}(\Omega) \big[\frac{N}{A}\delta\rho^p_\nu - \frac{Z}{A}\delta\rho^n_\nu\big] , \tag{2}$$

$T = 0$ toroidal

$$\begin{aligned}\langle\nu|\, \hat{M}^{\mathrm{tor}}_{1\mu}(T=0)\, |0\rangle &= -\frac{1}{10c\sqrt{2}} \int d\vec{r}\, r^3 \vec{Y}_{11\mu}(\Omega_i)\cdot(\nabla\times\delta\vec{j}_\nu) \\ &= -\frac{i}{2c\sqrt{3}} \int d\vec{r}\, \delta\vec{j}_\nu \cdot \big[\frac{\sqrt{2}}{5} r^2 \vec{Y}_{12\mu}(\Omega) + (r^2 - \langle r^2\rangle_0)\vec{Y}_{10\mu}(\Omega)\big] ,\end{aligned} \tag{3}$$

and $T = 0$ compression

$$\begin{aligned}\langle\nu|\, \hat{M}^{\mathrm{com}}_{1\mu}(T=0)\, |0\rangle &= -i\frac{1}{10c} \int d\vec{r}\, r^3 Y_{1\mu}(\Omega)(\nabla\cdot\delta\vec{j}_\nu) \\ &= -i\frac{1}{2c\sqrt{3}} \int d\vec{r}\, \vec{j}_\nu \cdot \big[\frac{2\sqrt{2}}{5} r^2 \vec{Y}_{12\mu}(\Omega) - (r^2 - \langle r^2\rangle_0)\vec{Y}_{10\mu}(\Omega)\big].\end{aligned} \tag{4}$$

In Eqs. (3) and (4), the terms with the ground state square radius $\langle r^2 \rangle_0$ represent center-of-mass corrections [14, 37]. Eq. (2) includes the familiar effective charges $(N/A\ ,\ -Z/A)$ and proton/neutron transition densities (TD) $\delta\rho^{\tau}_{\nu}(\vec{r}) = \langle\nu|\hat{\rho}^{\tau}|0\rangle(\vec{r})$ with $\tau = p, n$. Eqs. (3)-(4) include the convective transition currents (TC) $\delta\vec{j}_{\nu}(\vec{r}) = \langle\nu|\hat{\vec{j}}^{p} + \hat{\vec{j}}^{n}|0\rangle(\vec{r})$ [14].

The strength functions (1) are averaged by the Lorentz weight

$$\xi_{\Delta}(E - E_{\nu}) = \frac{1}{2\pi}\frac{\Delta(E)}{(E - E_{\nu})^2 + [\Delta(E)/2]^2} \tag{5}$$

with energy-dependent folding [36]

$$\Delta(E) = \begin{cases} \Delta_0 & \text{for} \quad E \le E_0, \\ \Delta_0 + a\,(E - E_0) & \text{for} \quad E > E_0. \end{cases} \tag{6}$$

We use the Lorentzian folding to simulate the escape width and coupling to the complex configurations (spreading width). Since these two effects grow with increasing excitation energy, we employ the energy dependent folding width $\Delta(E)$ with the parameters Δ_0 = 0.3 MeV, $E_0 = \min\{S_n, S_p\}$ MeV (with S_n and S_p being neutron and proton separation energies) and a =0.1667 [20].

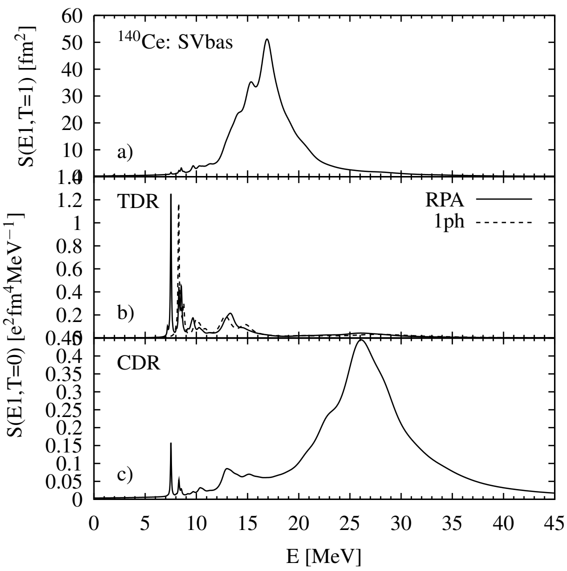

Figure 2. QRPA $E1$ strength functions (solid lines) in ^{140}Ce, calculated for: (a) IV GDR and PDR, (b) TDR, and (c) CDR. For TDR in panel (b), the 1ph strength (dotted line) is also depicted.

3 Results and Discussion

Our QRPA results are shown in Figures 2–5. In Figure 2, the energy-weighted dipole strength function ($X = \mathrm{el}$) (panel (a)) is compared with $T = 0$ TDR (panel (b)) and CDR (panel (c)) strength functions. Panel (a) demonstrates the isovector giant dipole resonance (IV GDR) with the maximum at $E \sim 12$ MeV and PDR at 7–11 MeV. Following panel (b), the TDR is peaked just in the PDR energy region. The TDR is formed already in 1ph case. The residual interaction downshifts and slightly enforces it. Following panel (c), some irrotational CDR strength exists at the PDR region as well. So dipole states at 7–11 MeV should have both vortical and irrotational fractions.

This is confirmed by the averaged transition densities (TD) and transition current (TC) shown in Figures 3–5. TD and TC are averaged over all the dipole states at the energy interval 7.0-10.4 MeV, using the prescription [15]. We do need the averaging to suppress individual details of the states (which can significantly vary from state to state) and highlight their common features. Figure 3 shows the averaged proton and neutron TD in QRPA and 1ph calculations. We see that, in 1ph case (panel (b)), the neutron TD slightly dominates the proton one at the nuclear surface. QRPA significantly increases this effect. Note that TD are determined by irrotational nuclear flow. So, Figure 3 confirms that dipole states at 7–11 MeV have some irrotational fraction.

However, the major fraction of these states is vortical. This follows from Figure 4, where proton, neutron, $T = 0$ and $T = 1$ averaged TC calculated within QRPA are shown. We see that nuclear flow at 7.0–10.4 MeV is mainly isoscalar and, what is most important, is basically of the vortical toroidal character (to be compared with the schematic picture in Figure 1(a)). Further, Figure 5 indicates that toroidal flow: i) exists already in 1ph TC, i.e. is of the mean-field origin (in accordance with previous findings in Refs. [18, 26, 38]), ii) is mainly produced by neutrons. So, in dipole states at 7.0-10.4 MeV, both major vortical (TDR) and minor irrotational (PDR) fractions coexist.

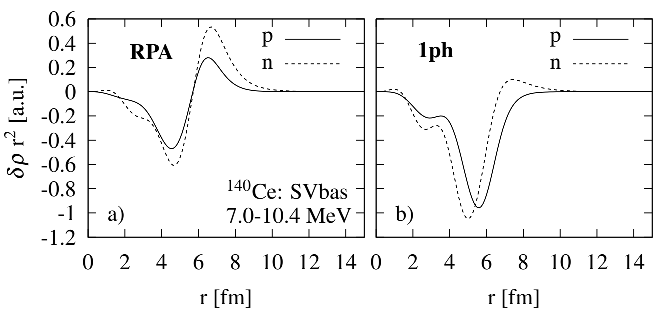

Figure 3. The averaged QRPA (left) and 1ph (right) proton (solid line) and neutron (dotted line) transition densities in ^{140}Ce, calculated for dipole states at 7.0-10.4 MeV.

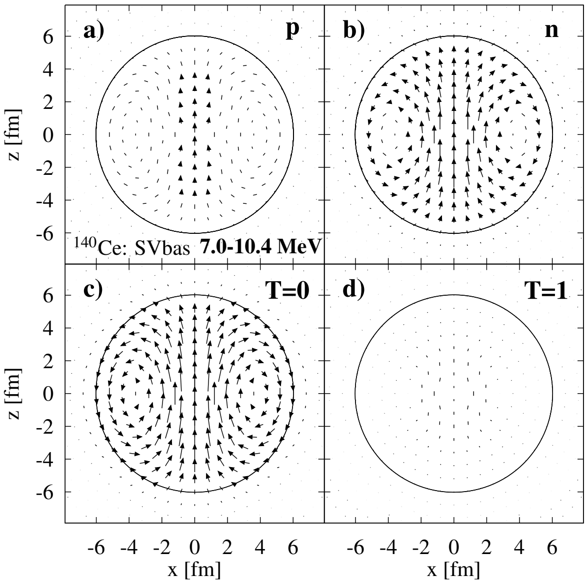

Figure 4. The averaged QRPA convection nuclear currents in ^{140}Ce, calculated for dipole states at 7.0-10.4 MeV: (a) proton, (b) neutron, (c) isocalar (T=0), and (d) isovector (T=1).

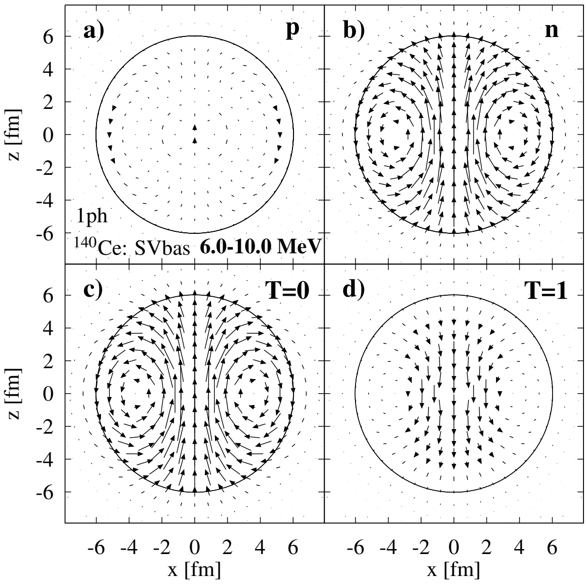

Figure 5. The as in Figure 4. but for 1ph excitations at 6.0–10.0 MeV.

Note that, in calculation of TD and TC, we do not use any toroidal or compression transition operators. Both TD and TC are fully determined by wave functions of the involved dipole states. So the coexistence of the major toroidal and minor irrotational fractions is just the inherent feature of the involved states.

Finally note that PDR exists only in nuclei with a neutron excess while TDR should take place in all atomic nuclei (for exception of very small nuclei where the mean-field conception is already not valid). Indeed, in all the nuclei, there is a bunch of unperturbed 1ph dipole strength generated by 1ph $E1$ transitions between the neighbor shells. The bunch energy is $E_{\rm 1ph} \approx 41A^{-1/3}$ MeV [2]. This 1ph dipole strength has both irrotational and vortical fractions. The repulsive $E1(T=1)$ residual interaction upshifts the irrotational strength to form the isovector GDR. However this interaction does not much affect $T=0$ strength, especially its vortical fraction. So a large part of the vortical strength remains at $E_{\rm 1ph}$ and becomes even dominant there, thus forming the TDR [26].

4 Conclusions

The interplay of the vortical toroidal dipole resonance (TDR) and irrotational pygmy dipole resonance (PDR), sharing the same energy region, was analyzed within fully self-consistent quasiparticle random-phase-approximation method (QRPA) [20] with the Skyrme force SVbas [34]. We scrutinized dipole strength functions, transition densities and distributions of the nuclear current in the spherical nucleus ^{140}Ce.

It was shown that dipole states at the energy region of our interest have major vortical (TDR) and minor irrotational (PDR) fractions. The former fraction gives basically toroidal distribution of the nuclear current while the latter produces a typical PDR behavior of the transition densities. So we have a coexistence of two very different nuclear modes (TDR and PDR) at the same energy region.

Both modes are of a significant interest. PDR is important for various astrophysical applications and building of the nuclear equation of state while TDR is a remarkable example of the vortical nuclear flow beyond the continuity equation. The TDR/PDR interplay can in principle affect both modes and so is of primary interest. The PDR fraction can be used as a doorway in an experimental search of TDR.

Acknowledgements

We are grateful to A. Repko for his codes and numerical results presented in this paper. We thank Prof. P.-G. Reinhard for fruitful discussions. The work was partly supported by Votruba – Blokhintsev (Czech Republic - BLTP JINR) grant. J.K. thanks the grant of Czech Science Agency (Project No. 19-14048S).

References

[1] P. Ring and P. Schuck, *The Nuclear Many-Body Problem* (Springer-Verlag, Berlin, 1980).

[2] M.N. Harakeh and A. van der Woude, *Giant Resonances* (Clarendon Press, Oxford, 2001).

[3] N. Lo Iudice and F. Palumbo, *Phys. Rev. Lett.* **4**1 (1978) 1532.

[4] R.R. Hilton, *Z. Phys. A* **3**16 (1984) 121.

[5] G. Holzward and G. Ekardt, *Z. Phys. A* **2**83 (1977) 219.

[6] S.F. Semenko, *Sov. J. Nucl. Phys.* **3**4 (1981) 356.

[7] S.I. Bastrukov, Ş. Mişicu, and A.V. Sushkov, *Nucl. Phys. A* **5**62 (1993) 191.

[8] Ş. Mişicu, *Phys. Rev. C* **7**3 (2006) 024301.

[9] E.B. Balbutsev, I.V. Molodtsova, and A.V. Unzhakova, *Europhys. Lett.* **2**6 (1994) 499.

[10] N. Ryezayeva, T. Hartmann, Y. Kalmykov, H. Lenske, P. von Neumann-Cosel, V. Yu. Ponomarev, A. Richter, A. Shevchenko, S. Volz, and J. Wambach, *Phys. Rev. Lett.* **8**9 (2002) 272502.

[11] G. Colo, N. Van Giai, P.F. Bortignon, and M.R. Quaglia, *Phys. Lett. B* **4**85 (2000) 362.

[12] D. Vretenar, N. Paar, P. Ring, and T. Nikšić, *Phys. Rev. C* **6**5 (2002) 021301(R).

[13] N. Paar, D. Vretenar, E. Khan, G. Colo, *Rep. Prog. Phys*. **7**0 (2007) 691.

[14] J. Kvasil, V.O. Nesterenko, W. Kleinig, P.-G. Reinhard, and P. Vesely, *Phys. Rev. C* **8**4 (2011) 034303.

[15] A. Repko, P.-G. Reinhard, V.O. Nesterenko, and J. Kvasil, *Phys. Rev. C* **8**7 (2013) 024305.

[16] P.-G. Reinhard, V.O. Nesterenko, A. Repko, and J. Kvasil, *Phys. Rev. C* **8**9 (2014) 024321.

[17] J. Kvasil, V.O. Nesterenko, W. Kleinig, and P.-G. Reinhard, *Phys. Scr.* **8**9 (2014) 054023.

[18] V.O. Nesterenko, A. Repko, P.-G. Reinhard, and J. Kvasil, *EPJ Web of Conferences*, **9**3 (2015) 01020.

[19] V.O. Nesterenko, J. Kvasil, A. Repko, W. Kleinig, P.-G. Reinhard, *Phys. Atom. Nucl.* **7**9 (2016) 842.

[20] A. Repko, J. Kvasil, V.O. Nesterenko, and P.-G. Reinhard, *Eur. Phys. J. A* **5**3 (2017) 221.

[21] V.O. Nesterenko, A. Repko, J. Kvasil, and P.-G. Reinhard, *Phys. Rev. Lett.* **1**20 (2018) 182501.

[22] V.O. Nesterenko, J. Kvasil, A. Repko, and P.-G. Reinhard, *Eur. Phys. J. Web of Conf.* **1**94 (2018) 03005.

[23] D.H. Youngblood, Y.-W. Lui, B. John, Y. Tokimoto, H.L. Clark, and X. Chen, *Phys. Rev. C* **69**, 054312 (2004).

[24] M. Uchida, et al, H. Sakaguchi, M. Itoh, M. Yosoi, T. Kawabata, Y. Yasuda, H. Takeda, T. Murakami, S. Terashima, S. Kishi, U. Garg, P. Boutachkov, M. Hedden, B. Kharraja, M. Koss, B.K. Nayak, S. Zhu, M. Fujiwara, H. Fujimura, H.P. Yoshida, K. Hara, H. Akimune, and M.N. Harakeh, *Phys. Rev. C* **69**, 051301(R) (2004).

[25] V.O. Nesterenko, A. Repko, J. Kvasil, and P.-G. Reinhard, *Phys. Rev. C* **100** (2019) 064302.

[26] A. Repko, V.O. Nesterenko, J. Kvasil, and P.-G. Reinhard, *Eur. Phys. J. A* **55** (2019) 242; arXiv:1903.01348[nucl-th].

[27] A. Repko and J. Kvasil, *Acta Phys. Polon. B Proceed. Suppl.* **1**2 (2019) 689; arXiv:1904.11259 [nucl-th].

[28] Y. Kanada-En'yo and Y. Shikata, *Phys. Rev. C* **9**5 (2017) 064319.

[29] Y. Shikata, Y. Kanada-En'yo, and H. Morita, *Prog. Theor. Exp. Phys.* (2019) 063D01.

[30] Y. Kanada-En'yo, Y. Shikata, and H. Morita, *Phys. Rev. C* **9**7 (2018) 014303 .

[31] Y. Kanada-En'yo and Y. Shikata, *Phys. Rev. C* **1**00 (2019) 014301.

[32] Y. Kanada-En'yo and H. Horiuchi, *Front. Phys.* **1**3 (2018) 132108.

[33] M. Bender, P.-H. Heenen, P.-G. Reinhard, *Rev. Mod. Phys.* **7**5 (2003) 121.

[34] P. Klüpfel, P.-G. Reinhard, T.J. Burvenich, and J.A. Maruhn, *Phys. Rev. C* **7**9 (2009) 034310.

[35] M. Bender, K. Rutz, P.-G. Reinhard, J.A. Maruhn, *Eur. Phys. J. A* **8** (2000) 59.

[36] J. Kvasil, V.O. Nesterenko, W. Kleinig, D. Bozik, P.-G. Reinhard, and N. Lo Iudice, *Eur. Phys. J. A* **49**, (2013) 119 .

[37] A. Repko, J. Kvasil, and V.O. Nesterenko, *Phys. Rev. C* **9**9 (2019) 044307.

[38] D.G. Raventhall, J. Wambach, *Nucl. Phys. A* **475** (1987) 468.